

Comparative evaluation of centralized and decentralized solar street lighting systems

Kenzie Joviancent, Levin Halim, Christian Fredy Naa

Department of Electrical Engineering, Faculty of Industrial Technology, Universitas Katolik Parahyangan, Bandung, Indonesia

Article Info

Article history:

Received Mar 20, 2024

Revised Jun 19, 2024

Accepted Jul 1, 2024

Keywords:

Energy efficiency

Power loss

Solar street lighting

Urban infrastructure

Voltage drops

ABSTRACT

Inadequate lighting can hinder outdoor activities such as traffic or pedestrian access. Solar street lighting system is planned to provide sufficient lighting for roads lacking proper illumination. DIALux software uses simulation to determine the lamp power and pole specifications, followed by applying formulas to establish component specifications. In this research, a performance comparison based on voltage drop and power losses will be conducted for solar street lighting systems with decentralized and centralized systems. With a road length of 130 meters and a width of 5 meters, simulations were performed for each variable of lamps (10, 12, 19, and 30 Watt). The calculations show that 4 streetlights are needed, and simulation results indicated that the most suitable lamp power is 12 Watt. The analysis showed that the centralized and decentralized designs do not have voltage drops exceeding the applicable limit. However, the centralized design has higher power losses amounting to 3.68 Watt. Another advantage of the decentralized design is its independence, with each load powered by a separate solar panel, while the centralized design is vulnerable to the overall system. In conclusion, the decentralized design is more suitable for implementation after comparing the centralized and decentralized designs based on the voltage drop and power losses.

This is an open access article under the [CC BY-SA](https://creativecommons.org/licenses/by-sa/4.0/) license.



Corresponding Author:

Levin Halim

Department of Electrical Engineering, Faculty of Industrial Technology, Universitas Katolik Parahyangan
Ciumbuleuit Street No.94, Hegarmanah, Bandung, West Java 40141, Indonesia

Email: halimlevin@unpar.ac.id

1. INTRODUCTION

Electrical energy is a fundamental form of energy that functions as the primary source of power for a wide range of processes, including but not limited to electrical, thermal, and other associated activities [1]–[3]. The capacity to execute tasks specifically utilized in electrical applications [4]. At the national level, most countries have initiated the implementation of sustainable development goals (SDGs). These endeavors are recorded in the early voluntary national reviews (VNRs) submitted to the high-level political forum for sustainable development (HLPF) in 2016 and 2017 [5]. To avoid being left behind, the Indonesian government has committed to and agreed to reduce the consumption of fossil fuels, opting for a more affordable transition to renewable energy [6]–[9]. The feasibility of implementing solar power plants in Indonesia is significantly supported by several factors, including the country's extensive reservoir lands, current regulatory framework, and its geographical location near the equator with a tropical climate [10]–[12]. Indonesia has made significant progress utilizing solar energy [13], [14]. One example is the floating solar power plant on the Cirata reservoir [15], [16].

A realistic alternative that utilizes solar energy is the implementation of a solar street lighting system [17]–[19]. Nevertheless, the significant constraints in implementing such systems include cost,

maintenance, and efficiency challenges. On the other hand, determining the optimal number of lighting spots and the appropriate lamp power to illuminate all road parts remains unclear. Currently, most streetlights are manually switched, resulting in occasional mistimed switching owing to human mistakes. Consequently, lamps may remain illuminated during daylight hours. Hence, time-based lamps are employed to activate and deactivate at precise intervals. However, this approach is hindered by the seasonal variations in sunset and rising times [18].

This research addresses the uncertainty in determining the most suitable decentralized or centralized design. It also aims to establish the optimal number of lighting spots and appropriate lamp power to illuminate all parts of a road. The study involved the development of two different schemes for solar street lighting systems: a decentralized system (design 1) and a centralized system (design 2). The research location is in Bandung, Indonesia.

A comparison will be made between decentralized and centralized solutions using exact calculated lamp specifications. Furthermore, this research aims to determine the specifications of each component as well as calculate the voltage drops and power losses in each component connection. These values will then be compared to the relevant regulatory standards. The Institution of Engineering and Technology has released British standard (BS) 7671, which outlines the specifications for electrical installations [20]. This standard specifies the permissible voltage drop that must be maintained from the supply point to any given location within the system. The voltage drop calculation is frequently performed to mitigate the risk of excessive potential difference across the load [20], ensuring efficient operation by minimizing the potential difference.

The design framework will adhere to the governmental rules specified in the Indonesian national standard (SNI) 7391:2008, which pertains to the criteria for street lighting in metropolitan areas [21]. After the road categorization has been aligned with the requirements set by the SNI, the variable values are recorded and subsequently utilized as experimental variables in the DIALux simulation. After thorough calculations and DIALux simulations to identify and evaluate all aspects that impact the design, a comparative analysis will be performed between the decentralized and centralized systems of this solar street lighting system.

2. METHOD

The research was initiated by determining the value of the lamp used and the extent of the road length that this lamp will illuminate. In this research, the specification of the road length is set at 130 meters with a width of 5 meters. The following steps were taken:

- Component specifications determination: The values of the lamp power, distance between poles, and pole height were determined. These values were then input into the DIALux software, a tool widely used for lighting design and simulation, to assess luminance, illumination, and glare threshold values. DIALux settings included a pole height of 4 meters and an E27 lamp model with a beam angle of 40 degrees.
- Simulation: Simulations were conducted using DIALux for different lamp wattages (10, 12, 19, and 30 Watt) at varying pole-to-pole distances (29, 30, and 32 meters). The average luminance results were matched with the values in Table 1 for local road classification, aiming for E_{avg} values within the range of 2-5 Lux. These simulation results were compared with the Indonesian National Standard (SNI) 7391:2008 requirements to find the most suitable lamp power values for the researched road classification.
- Calculations: The total number of lighting points required was calculated. Also, the road length was determined using google maps, which provided precise measurement points.
- Energy load and solar module capacity: The daily energy load for each lighting point was calculated. This load was then used to determine the required solar module capacity.
- Battery and controller specifications: The battery capacity was determined. On the other hand, the solar charge controller (SCC) capacity was also calculated.
- Voltage drops and power losses: Voltage drop calculations were performed. Cable resistivity values were taken from standard tables (e.g., Table 1 for resistivity of common conductors). Also, the power losses were calculated. The results were compared to ensure they met the British Standard (BS) 7,671 requirements for permissible voltage drop.

In Table 2, each road will be further classified based on the required lighting quality. Roads in this research are classified based on their function and location using the definition of local roads, a public road serving local transportation with characteristics of short-distance travel, low average speed, and an unrestricted number of entrances [21]. Therefore, all variables for primary local roads are utilized in the design. To determine the ideal distance between poles, the road width, type, and height values of lamps are matched according to the conditions and desired values based on Table 3.

Table 1. Resistivity of common conductors

Road type/Classification	Illuminance		$L_{average}$ (cd/m^2)	Luminance		Glare limitation	
	E_{avg} (lux)	Uniformity U_o		Uniformity VD	Uniformity VI	G	TJ (%)
Sidewalk	1 – 4	0.10	0.10	0.40	0.50	4	20
Local Road:	2 – 5	0.10	0.50	0.40	0.50	4	20
- Primary	2 – 5		0.50	0.40	0.50	4	20
- Secondary							
Collector Road:	3 – 7	0.14	1.00	0.40	0.50	4 – 5	20
- Primary	3 – 7		1.00	0.40	0.50	4 – 5	20
- Secondary							
Arterial Road:	11 – 20	0.14 – 0.20	1.50	0.40	0.50 – 0.70	5 – 6	10 – 20
- Primary	11 – 20	0.14 – 0.20	1.50	0.40	0.50 – 0.70	5 – 6	10 – 20
- Secondary							
Arterial Road with controlled access	15 – 20	0.14 – 0.20	1.50	0.40	0.50 – 0.70	5 – 6	10 – 20
Flyover, stack interchange, tunnel	20 – 25	0.20	2.00	0.40	0.70	6	10

Table 2. Normal lighting quality [21]

Lamp classification	Lamp height (m)	Road Width (m)									Brightness
		4	5	6	7	8	9	10	11		
35 W SOX	4	32	32	32							3.5 LUX
	5	35	35	35	35	34	32	-			
	6	42	40	38	36	33	31	30	29		
55 W SOX	6	42	40	38	36	33	32	30	28	6.0 LUX	
90 W SOX	8	60	60	58	55	52	50	48	46	10.0 LUX	
90 W SOX	8	36	35	35	33	31	30	29	28		
135 W SOX	10	46	45	45	44	43	41	40	39	20.0 LUX	
135 W SOX	10	-	-	25	24	23	22	21	20		
180 W SOX	10	-	-	37	36	35	33	32	31		
180 W SOX	10	-	-	-	-	22	21	20	20	30.0 LUX	

Table 3. Light distribution [21]

Material	Resistivity		
	$\mu\Omega m$	$\mu\Omega cm$	$\mu\Omega mm$
Copper (annealed)	0.0172	1.72	17.2
Copper (hard-drawn)	0.0178	1.78	17.8
Aluminum	0.0285	2.85	28.5
Tin	0.114	11.4	114
Lead	0.219	21.9	219
Mercury	0.958	95.8	958
Iron	0.100	10.0	100
Silver	0.0613	1.63	16.3
Brass	0.06 – 0.09	6 – 9	60 – 90

Then, to determine the required lighting points for a road, it is used (1) for calculation:

$$T = \frac{L}{s} \quad (1)$$

where T is the total number of lighting points, L is the overall length of the road (meter), and s is the distance between poles (m). The length of the road can be determined through manual calculations or by using the functions on Google Maps to pinpoint the measured road with the starting and ending points. Google Maps will automatically display the length of that road.

Light emitting diode (LED) is one type of lamp that can save energy consumption. LEDs convert electrical energy into light energy [22]. The power of the lamp used will be a variable that determines the total daily load. After obtaining the lamp power values based on matching the DIALux simulation results with the required values according to SNI 7391:2008, the daily load for each lighting point is determined using (2) [23].

$$E_T = P_L t \quad (2)$$

where E_T is the total load (Watt), P_L is the power of the used lamp (Watt), and t is the operating time of the lamp (hour). The total load is required for further calculations to determine the solar module capacity that can power the total daily load so that the system can operate effectively.

Determining solar module capacity requires the research location's total solar radiation value or global horizontal irradiance (GHI). Solar radiation value (GHI) is determined using the website [24]. After obtaining the solar radiation value, to determine the minimum capacity of the required solar panel, use (3) [25].

$$D_{SOLARCELL} = \frac{E_T}{G} \quad (3)$$

where $D_{SOLARCELL}$ is the capacity of the solar panel, E_T is the exact total load for the equation before (Watt), and G is the variable of global horizontal irradiation ($\text{kWh}/\text{m}^2/\text{day}$).

In batteries, there is also a specification known as depth of discharge (DOD), where this variable determines the percentage of battery capacity used. DOD will affect the battery lifespan and is an important variable that needs attention because the battery is the most expensive component in off-grid solar power systems. The formula to determine the battery capacity in the system is shown in (4).

$$D_{BATT} = \frac{E_T(AD)}{DOD(V_S)} \quad (4)$$

where AD is the autonomous day for the system to continue operating smoothly even if the solar panel is not charging the battery because the battery already contains sufficient power for the system to function for several days without any power input from the solar panel (day), DOD is the percentage of some portion of the battery's 100% capacity (%), and V_S is the voltage source system (V).

After determining all component values, a controller must regulate the voltage flow for each solar-powered public street lighting system connection. Therefore, a solar charge controller (SCC) is needed. The specifications of the SCC are calculated using (5),

$$D_{SCC} = \frac{D_{SOLARCELL}}{V_S} \quad (5)$$

where D_{SCC} is the capacity of the solar charge controller, $D_{SOLARCELL}$ is the capacity of the solar panel from (5).

The use of electronic devices that operate with alternating current (AC), such as the lamps that will be used in the solar-powered public street lighting system, requires a device that can convert direct current (DC) from solar panels and batteries into alternating current (AC) [26]. The last component, the inverter, converts DC electrical current from the battery into AC to be supplied to the AC load, namely the lamps. To determine the inverter capacity, the inverter power must be greater than the maximum load power. The mathematical formula can be seen in (6) [26].

$$P_{in} > P_{maxload} \quad (6)$$

where P_{in} is the inverter power and $P_{maxload}$ is the maximum load power. The results obtained from (6) will be adjusted to the specifications available in the industry or market. In this final project design, the inverter component will be used as a DC converter the battery provides through the SCC into AC to power LED lights.

The decentralized and centralized system's design will be compared based on cable voltage drop and the power dissipation for the cables connected to each component. After obtaining the simulation results, the recorded power values of the used lamps will be noted. After obtaining the simulation results, the power values of the used lamps are evaluated. The system will be inefficient with such a low applied voltage. For this reason, BS 7671 limits the maximum allowable voltage drop in the system to 4% of the supply voltage [20]. For the cable type resistance for voltage drop calculations, please refer to Table 3.

The voltage drop calculation is crucial for determining the specifications of cables that match the voltage and current values, aiming to prevent excessive heating or even fires within the system. Since voltage can be expressed by multiplying current with resistance ($V = IR$), the voltage drop in the cable depends on the carried current and its resistance. This, in turn, is influenced by the conductor material, cable length, cross-sectional area, and cable temperature [20]. The formula for cable resistance can be seen in (7).

$$\text{Cable Resistance } (R) = \frac{\rho l}{A} \quad (7)$$

where R is the cable resistance, ρ is the resistivity of the conductor material, l is the cable length, and A is the cross-sectional area of the cable used. After obtaining the cable resistance values, the cross-sectional area of the cable is required, where the conductor area is inside the cable through which the current flows. The value of this area is shown in Table 4 and adjusted according to the size of the cable used.

Table 4. Conductor trade sizes [27]

AWG	mm ²	AWG	mm ²
18	0.823	3	26.67
16	1.31	2	33.62
14	2.08	1	42.41
12	3.31	1/0	53.49
10	5.261	2/0	67.43
8	8.367	3/0	85.01
6	13.30	4/0	107.2
4	21.15		

Knowing how much power an electrical device can handle is necessary for practical purposes. Therefore, power and energy calculations become essential in analyzing electrical circuits using (8).

$$P = VI \tag{8}$$

where V is the system voltage, and I is the system current. Then (8) is substituted using Ohm's law to find the power losses generated by the circuit, becoming (9).

$$P_{loss} = I^2R \tag{9}$$

where I is the current flowing through the system in ampere (A), and R is the resistance between connected components (Ω).

3. RESULTS AND DISCUSSION

Based on a direct inspection of the research object, namely the entrance road where lighting fixtures will be installed, the results are obtained as shown in Table 5. The road length is 130.67 meters, based on measurement points from Google Maps in Figure 1 and 5 m, based on manual field survey measurement. These measurements are critical as they determine the number and spacing of the lighting fixtures. Ensuring accurate measurements allows for a reliable comparison between the decentralized and centralized lighting systems, highlighting the efficiency and effectiveness of each design. On the other hand, the road classifications are regional and national, which usually fall into the category of primary arterial roads that connect cities and provinces.

Table 5. Technical data of the road

Description	Specification	Description	Specification
Road length	130 m	Road status	Regional
Road width	5 m	Road function	Local
Number of lanes	2 Lanes; 1 way	Road class	Primary



Figure 1. Measured length of the road observation on Google Maps

Subsequently, simulations were conducted in DIALux with lamp variables of 10, 12, 19, and 30 Watt simulated at 29, 30, and 32 meters. The average luminance results were matched with the values in Table 1 for local road classification, aiming for E_{avg} values within the range of 2-5 Lux. Using a pole height setting of 4 meters and an E27 lamp model with a boom angle of 40 degrees, the simulation results are presented in Table 6. These simulations provide critical insights into the appropriate wattage and spacing for optimal lighting.

The results from the DIALux simulation with a pole-to-pole distance of 29, 30, and 32 meters can be seen in Table 6, with various lamp variables. For the 29 meter pole-to-pole distance, the value to be noted is E_{avg} , with a value of 2 Lux, chosen within the range specified in Table 1 for local roads, which is 2-5 Lux. The minimum value is selected to ensure that the power of the lamp used is not too high, thus reducing design costs and uniformity (U_o) > 0.10 Lux. It can be seen in Table 6 that the lamp power closest to this value is 12 Watt, with an E_{avg} of 2.17 Lux and a uniformity of 0.12. This indicates that a 12 Watt lamp at a 29 meter pole-to-pole distance provides adequate lighting while minimizing energy use. This setup ensures sufficient road illumination, contributing to safer night-time visibility. These findings support previous research that emphasized the efficiency of lower-wattage lamps for urban lighting [19].

Table 6. Results of the DIALux simulation

Lamp (Watt)	Lumen	Lamp's height (m)	Distance between poles (m)	E_{avg} (Lux)	E_{min} (Lux)	L_{avg} (Cd/m ²)	Uo	Ti (%)
Illuminance								
10	1020	4	29	1.63	0.19	0.13	0.11	43
12	1360			2.17	0.26	0.18	0.12	46
19	2300			4.03	0.40	0.30	0.10	44
30	3200			5.38	0.61	0.43	0.11	50
10	1020	4	30	1.58	0.17	0.13	0.11	42
12	1360			2.10	0.24	0.17	0.09	45
19	2300			3.89	0.36	0.29	0.11	43
30	3200			5.20	0.55	0.42	0.11	50
10	1020	4	32	1.48	0.13	0.12	0.09	42
12	1360			1.97	0.18	0.16	0.09	45
19	2300			3.65	0.28	0.27	0.08	43
30	3200			4.88	0.42	0.39	0.09	49

Then, a pole-to-pole distance of 30 meters was simulated to compare the values of E_{avg} and uniformity produced with different pole-to-pole distances to find the optimal pole-to-pole distance for each compared lamp power. It is noted that for a pole-to-pole distance of 30 meters, the value closest to 2 Lux is also 12 Watt, with an E_{avg} value of 2.19, which is 0.07 smaller than the previous result, and a uniformity (U_o) of 0.09. From the comparison of these two values, the 12 Watt lamp with a pole-to-pole distance of 29 meters are selected. On the other hand, the results for a pole-to-pole distance of 32 meters do not have a value close to 2 Lux within the range of 2 - 5 Lux, so no comparison of values is involved.

Applying the formulas in the Method section, specifications for each component of both designs were obtained for comparison. The sun radiation (GHI) value for the area with coordinates -06.877289°, 107.610712° is 4.615 kWh/m²/day, with a voltage source voltage of 12 Volt, and the system will operate for 12 hours with the assumption that the solar panel is optimally illuminated for 4 hours, from 10.00 AM to 02.00 PM.

Referring to Table 7, the results obtained for design 1 (decentralized) indicate that each lighting point requires a 35 Wp solar panel and a 45 Ah battery. Each lighting point will be powered by 1 solar panel and other supporting components for the decentralized system. Therefore, there will be 4 solar panels for design 1 (decentralized), while for design 2 (centralized), there will be only 1 solar panel with a size of 135 Wp and a battery size of 180 Ah. This research's component specifications align with the findings of [19], highlighting decentralized systems' scalability. By independently powering each lighting point, decentralized systems can be easily expanded or modified based on specific urban requirements, adding to the flexibility and robustness of urban lighting solutions.

All the required component specifications were obtained in the calculation with a result in Table 7, and both designs of solar street lighting were established for comparison. For design 1, each lighting point will be powered by its respective solar panel. In decentralized and centralized design, the length of each cable connected is in Table 8.

Table 7. List of components

	Design 1 (decentralized)	Design 2 (centralized)
Number of poles		4 poles
Solar Panel	35 Wp	125 Wp
Battery	45 Ah; 12 V	180 Ah; 12 V
SCC	10 A	20 A
Inverter		150 Watt

Table 8. List of connections between components

Design 1 (decentralized)					Design 2 (centralized)				
Name	Component connection	Cable's length (m)	Cable's Quantity	Total length (m)	Name	Component connection	Cable's length (m)	Cable's Quantity	Total length (m)
D1.1	Solar panel → SCC	3	2	6	D2.1	Solar panel → SCC	3	2	6
D1.2	SCC → Battery	0.5		1	D2.2	SCC → Battery	0.5		1
D1.3	SCC → Photocell	3		6	D2.3	SCC → Photocell sensor	3		6
D1.4	Photocell → Inverter	3		6	D2.4	Photocell sensor → Inverter	3		6
D1.5	Inverter → Lamp	2.5		5	D2.5	Inverter → Busbar	0.5		1
					D2.6	Lamp 4 → Busbar	92		184
					D2.7	Lamp 3 → Busbar	63		126
					D2.8	Lamp 2 → Busbar	34		68
					D2.9	Lamp 1 → Busbar	5		10

Table 8 lists the connection between components in the decentralized design, which means the total length of 24 m in Table 8 is just for one lighting point. The total number of lighting points required after calculation with a road length of 130 meters and a width of 5 meters is 4 lighting points. This means the total cable needed for a Decentralized design is 24 m times 4 lighting points, which is 96 m. Consider the current output from each component multiplied by a 1.5 safety factor (SF) for the cable size used in the decentralized design. For the decentralized design with a 35 Wp solar panel, the peak current at maximum power (I_{mp}) is 1.97 A \approx 2 A, so the system output for the cable connection between the solar panel and SCC is 2 A \times 1.5 SF = 3 A and current output system for components connection between SCC 10 A and battery is 10 A \times 1.5 SF = 15 A. Referring to the National Electric Code (NEC), a 14 American wire gauge (AWG) cable size can carry a current of up to 20 A [28].

Whereas for the centralized design, all listed components will be used a cable size of 10 AWG with a current carrying capacity of 30-40 A because considering the current at maximum power (I_{MP}) of the 135 Wp solar panel for the centralized design is 6.88 A \approx 7 A, and multiplied by a 1.5 SF equals 10.5 A. Referring to the NEC, a 14 AWG cable size can carry a current of 30 - 40 A [28].

After obtaining the variables needed to calculate cable resistance, with a value of ρ 17.2 $\mu\Omega$ mm taken from Table 3, the cable cross-sectional area (A) is 2.08 mm^2 for 14 AWG (design 1) and 5.261 mm^2 for 10 AWG (design 2) as seen in Table 4, all these variable values are entered into (7). Then, the cable resistance (R) will be multiplied by the system current to obtain the voltage drop in that component connection using Ohm's Law, which can be seen in Table 9. The current value is the current leaving the system, for example, the short circuit current (I_{sc}) value on the solar panel. The result will be compared to see if the resulting voltage drop is within the criteria, $U < 4\%$, or exceeds the specified limit [20]. The results of the voltage drop calculations can be seen in Table 9.

Table 9. The cable resistance and voltage drop calculation results for each connection component

Design 1 (decentralized)						Design 2 (centralized)					
Design	Cable's length (mm)	Cable resistance (R) (Ω)	Current output system (A)	Drop voltage (Volt)	Percentage voltage drop (%)	Design	Cable's length (mm)	Cable resistance (R) (Ω)	Current output system (A)	Drop voltage (Volt)	Percentage (%)
D1.1	3000	0.024	3	0.072	0.6	D2.1	3000	0.01	10.5	0.105	0.875
D1.2	500	0.004	15	0.06	0.5	D2.2	500	0.02	30	0.06	0.5
D1.3	3000	0.024	1.5	0.036	0.3	D2.3	3000	0.01	6	0.06	0.05
D1.4	3000	0.024	1.5	0.036	0.3	D2.4	3000	0.01	6	0.06	0.05
D1.5	2500	0.02	0.08175	0.00163	0.0007	D2.5	500	0.002	0.32	0.0006	0.0003
						D2.6	92,000	0.3	0.32	0.0906	0.04
						D2.7	63,000	0.2	0.33	0.064	0.03
						D2.8	34,000	0.1	0.34	0.032	0.014
						D2.9	5	0.01	0.35	0.0032	0.0014

As shown in Table 9, the highest voltage drop value is at the connection from the solar panel to the SCC (D1.1), and the smallest is the connection from the inverter to the lamp (D1.5) at 0.0016 Volt. The difference in voltage drop values is influenced by the magnitude of the current output between component connections, the cable size, cable resistance, and the cable connecting the components. So, for the decentralized design, each component does not exceed the 4% voltage drop limit of the 12 Volt DC system and the 220 Volt AC system, which is 0.48 Volt for the DC system and 8.8 Volt for the AC system.

For the centralized design, the voltage drop value will be larger than the decentralized design because the I_{MP} value is more significant at 7 A, with a difference of 5 A compared to the decentralized design. The most significant voltage drop value is at the connection from the solar panel to the SCC (D2.1) at 0.105 Volt, while the smallest V_{drop} is at the connection from the lamp 1 to the busbar due to its proximity to other lamps mounted further from the solar panel pole. The power loss results for the decentralized and centralized design also can be seen in Table 10. These results further validate the observations by [17], which noted that centralized systems often suffer from higher voltage drops and power losses due to longer cable runs.

In decentralized design, for all component connections, the resulting power losses total 0.28 Watt, with the most significant power loss generated from the connection from the solar panel to the SCC, totaling 0.21 Watt. This is due to the output current of the system multiplied by the safety factor, squared, with the cable resistance based on formula (7), which depends on the cable resistivity, length, and cross-sectional area of the cable conductor.

Meanwhile, for the centralized design, the resulting power losses are more significant, totaling 3.685 Watt, with a difference of 3.475 Watt. This indicates that the centralized design performs worse in transmitting power between components, with larger cable ampacity values than the decentralized design. The connection from the SCC to the battery generates the most significant power losses, with power losses amounting to 1.8 Watt.

Previous research by Shupler [17] and Sutopo *et al.* [18] indicated that decentralized systems offer advantages in reliability and lower maintenance costs due to their independent operation. Our findings align with these studies by showing that the decentralized design had lower voltage drops and power losses. This detailed analysis adds to the existing knowledge by quantifying the efficiency benefits of decentralized systems, especially in urban settings like Bandung.

Table 10. The results of the power loss calculation

Section	Design 1 (decentralized)			Section	Design 2 (centralized)		
	Cable resistance (R) (Ω)	Output current system (A)	Power loss (P_{loss}) (Watt)		Cable resistance (R) (Ω)	Output current system (A)	Power loss (P_{loss}) (Watt)
D1.1	0.024	3	0.21	D2.1	0.01	11	1.1025
D1.2	0.004	1,5	0.009	D2.2	0.002	30	1.8
D1.3	0.024	1,5	0.054	D2.3	0.01	6	0.36
D1.4	0.024	0,08175	0.00016	D2.4	0.01	6	0.36
D1.5	0.02	0,08174	0.00013	D2.5	0.002	0.32	0.0002048
				D2.6	0.3	0.32	0,03072
				D2.7	0.2	0.32	0.02048
				D2.8	0.1	0.32	0.01024
				D2.9	0.01	0.32	0.001024
	Total		0.28	Total			3.6851688

4. CONCLUSION




The decentralized system requires a 35 Wp solar panel, 10 A solar charge controller, 45 Ah 12 V battery, and 150 Watt inverter. The centralized system needs a 135 Wp solar panel, 20 A solar charge controller, 180 Ah 12 V battery, and 150 Watt inverter. Both designs meet the maximum voltage drop criteria, which is most important, with design 1 (decentralized) having 0.072 Volt and design 2 (0.105 Volt). design 2 loses 3.68 Watt, while design 1 loses 0.27. design 2 (centralized) uses 10 AWG cables, so if adopted, the implementation cost will be higher than design 1. However, the decentralized system is independent at each lighting point; thus, damage only affects one point. The decentralized system design also maximizes power availability for each lamp by supporting each load with one solar panel, reducing power shortages. In contrast, centralized system inverter or primary component failures can damage the entire system connection. The decentralized system architecture improves power management and maintenance reliability and efficiency. For lighting solely, the decentralized design is cheaper and more efficient than the centralized version due to the solar panel's modest power and smaller wires. These findings suggest significant implications for urban infrastructure planning, particularly in adopting renewable energy

solutions, as decentralized solar street lighting systems offer a reliable, efficient, and scalable solution for urban areas, providing a framework for policymakers and urban planners to consider in sustainable urban lighting solutions, enhancing urban resilience and energy independence.




REFERENCES

- [1] A. J. M. Thomson, "Physical properties of electricity," *Journal of Minimally Invasive Gynecology*, vol. 20, no. 3, pp. 269–270, May 2013, doi: 10.1016/j.jmig.2013.02.006.
- [2] N. Armaroli and V. Balzani, "Towards an electricity-powered world," *Energy and Environmental Science*, vol. 4, no. 9, 2011, doi: 10.1039/c1ee01249e.
- [3] Y. Zhang, M. Xie, V. Adamaki, H. Khanbareh, and C. R. Bowen, "Control of electro-chemical processes using energy harvesting materials and devices," *Chemical Society Reviews*, vol. 46, no. 24, pp. 7757–7786, 2017, doi: 10.1039/c7cs00387k.
- [4] P. Albertus, J. S. Manser, and S. Litzelman, "Long-duration electricity storage applications, economics, and technologies," *Joule*, vol. 4, no. 1, pp. 21–32, Jan. 2020, doi: 10.1016/j.joule.2019.11.009.
- [5] C. Allen, G. Metternicht, and T. Wiedmann, "Initial progress in implementing the sustainable development goals (SDGs): a review of evidence from countries," *Sustainability Science*, vol. 13, no. 5, pp. 1453–1467, May 2018, doi: 10.1007/s11625-018-0572-3.
- [6] D. Adisaputro and B. Saputra, "Carbon capture and storage and carbon capture and utilization: what do they offer to Indonesia?," *Frontiers in Energy Research*, vol. 5, Mar. 2017, doi: 10.3389/fenrg.2017.00006.
- [7] D. Hartono and B. P. Resosudarmo, "The economy-wide impact of controlling energy consumption in Indonesia: An analysis using a Social Accounting Matrix framework," *Energy Policy*, vol. 36, no. 4, pp. 1404–1419, Apr. 2008, doi: 10.1016/j.enpol.2007.12.011.
- [8] A. Schwarz, "Low carbon growth in Indonesia," *Bulletin of Indonesian Economic Studies*, vol. 46, no. 2, pp. 181–185, Aug. 2010, doi: 10.1080/00074918.2010.503562.
- [9] I. Chandra Setiawan, Indarto, and Deendarlianto, "Quantitative analysis of automobile sector in Indonesian automotive roadmap for achieving national oil and CO2 emission reduction targets by 2030," *Energy Policy*, vol. 150, Mar. 2021, doi: 10.1016/j.enpol.2021.112135.
- [10] A. Asbayou, A. Aamoume, M. Elyaqouti, A. Ihlal, and L. Bouhouch, "Benchmarking study between capacitive and electronic load technic to track I-V and P-V of a solar panel," *International Journal of Electrical and Computer Engineering*, vol. 12, no. 1, pp. 102–113, Feb. 2022, doi: 10.11591/ijece.v12i1.pp102-113.
- [11] M. Hasan, W. H. Alhazmi, W. Zakri, and A. U. Khan, "Parameter estimation and control design of solar maximum power point tracking," *International Journal of Electrical and Computer Engineering*, vol. 12, no. 5, pp. 4586–4598, Oct. 2022, doi: 10.11591/ijece.v12i5.pp4586-4598.
- [12] M. S. Islami, T. Urnee, and I. N. S. Kumara, "Developing a framework to increase solar photovoltaic microgrid penetration in the tropical region: A case study in Indonesia," *Sustainable Energy Technologies and Assessments*, vol. 47, p. 101311, Oct. 2021, doi: 10.1016/j.seta.2021.101311.
- [13] D. F. Silalahi, A. Blakers, M. Stocks, B. Lu, C. Cheng, and L. Hayes, "Indonesia's Vast solar energy potential," *Energies*, vol. 14, no. 17, p. 5424, Aug. 2021, doi: 10.3390/en14175424.
- [14] A. F. Madsuha, E. A. Setiawan, N. Wibowo, M. Habiburrahman, R. Nurcahyo, and S. Sumaedi, "Mapping 30 years of sustainability of solar energy research in developing countries: Indonesia case," *Sustainability*, vol. 13, no. 20, Oct. 2021, doi: 10.3390/su132011415.
- [15] T. Sukmawan, H. Nursyahbani, H. D. Wahyudi, T. Gunawan, and A. A. Wijaya, "Technical study of developing floating photovoltaic 145 MWac power plant project In Cirata reservoir," *IOP Conference Series: Materials Science and Engineering*, vol. 1096, no. 1, p. 12120, Mar. 2021, doi: 10.1088/1757-899x/1096/1/012120.
- [16] E. Prasetyo, R. Ramadhan, and R. Wahono, "Impact of auto-reclosing on transmission to large-scale grid-connected PV system in Cirata," Sep. 2020. doi: 10.1109/ict-pep50916.2020.9249932.
- [17] M. Shupler, "Review for effect of a solar lighting intervention on fuel-based lighting use and exposure to household air pollution in rural Uganda: a randomized controlled trial," *Hindawi Limited*, Jan. 2022. doi: 10.1111/ina.12986/v2/review1.
- [18] W. Sutopo, I. S. Mardikaningsih, R. Zakaria, and A. Ali, "A model to improve the implementation standards of street lighting based on solar energy: a case study," *Energies*, vol. 13, no. 3, p. 630, Feb. 2020, doi: 10.3390/en13030630.
- [19] H. J. Han *et al.*, "An advanced lighting system combining solar and an artificial light source for constant illumination and energy saving in buildings," *Energy and Buildings*, vol. 203, Nov. 2019, doi: 10.1016/j.enbuild.2019.109404.
- [20] J. Whitfield, *Electrical craft principles, volume 2*. Institution of Engineering and Technology, 2008. doi: 10.1049/pbns034e.
- [21] BSN, "Specifications for street lighting in urban areas." (in Bahasa) *SNI 7391: 2008, Badan Standardisasi Nasional*, 2008.
- [22] Y. Miao *et al.*, "Stable and bright formamidinium-based perovskite light-emitting diodes with high energy conversion efficiency," *Nature Communications*, vol. 10, no. 1, Aug. 2019, doi: 10.1038/s41467-019-11567-1.
- [23] J. Hossain, N. A. Algeelani, A. H. H. Al-Masoodi, and A. F. A. Kadir, "Solar-wind power generation system for street lighting using internet of things," *Indonesian Journal of Electrical Engineering and Computer Science*, vol. 26, no. 2, pp. 639–647, May 2022, doi: 10.11591/ijeecs.v26.i2.pp639-647.
- [24] World Bank Group, "Global solar Atlas." *Globalsolaratlas*. <https://globalsolaratlas.info/map> (accessed Jul. 05, 2024).
- [25] B. A. Bhayo, H. H. Al-Kayiem, and S. I. Gilani, "Assessment of standalone solar PV-Battery system for electricity generation and utilization of excess power for water pumping," *Solar Energy*, vol. 194, pp. 766–776, Dec. 2019, doi: 10.1016/j.solener.2019.11.026.
- [26] N. Evalina, F. I. Pasaribu, and A. A. H., "The use of inverters in solar power plants for alternating current loads," *Britain International of Exact Sciences (BioEx) Journal*, vol. 3, no. 3, pp. 151–158, Sep. 2021, doi: 10.33258/bioex.v3i3.496.
- [27] J. M. Daly, "Changes in the 2002 national electrical code." doi: 10.1109/papcon.2001.952959.
- [28] Spike Electric, "NEC allowable ampacities of insulated conductors rated 0-2000 volts." Spikeelectric.com. Accessed: Jun. 05, 2024. [Online]. Available: <https://spikeelectric.com/pdf/R-ampacities.pdf>




BIOGRAPHIES OF AUTHORS

Kenzie Joviancent    is a dedicated student pursuing a degree in mechatronics engineering from Catholic Parahyangan University, Bandung. Currently actively researching renewable energy, mainly focusing on solar panel technologies and their application in infrastructure projects in Indonesia. He can be contacted at email: kenzie88jo@gmail.com.



Levin Halim    received a bachelor's degree in electrical power engineering and a master's degree in electrical engineering from the Bandung Institute of Technology in Indonesia in 2014 and 2015, respectively. Currently, they hold the position of assistant professor at the Department of Electrical Engineering at Parahyangan Catholic University. His research interests include renewable energy, power quality, power electronics, power generation, power grids, power supply quality, power transmission reliability, power transmission lines, power transmission planning, power transmission protection, battery chargers, circuit breakers, harmonic distortion, load flow control, power distribution protection, and the application of artificial intelligence in power systems. He can be contacted at email: halimlevin@unpar.ac.id.



Christian Fredy Naa    is a lecturer in the Department of Electrical Engineering at Parahyangan Catholic University. He holds a bachelor of science degree in physics from the prestigious Bandung Institute of Technology, earned in 2009. Further advancing his education, he acquired a master of science degree in 2011 from Kanazawa University, followed by a doctorate from Littoral University in 2017. Specializing in measurement and data acquisition as well as embedded systems, he contributes significantly to his field, combining academic rigor with practical expertise. He can be contacted at email: christian.fredy@unpar.ac.id.